



CHANGES IN PARTICLE BREAKAGE AND PENETRATION RESISTANCE OF GRAVELLY MUDSTONE DUE TO DRYING/WETTING AND TEMPERATURE CYCLES IN OEDOMETER TEST

Mohamed NIHAAJ¹, Takashi KIYOTA², Masataka SHIGA³, and Toshihiko KATAGIRI⁴

ABSTRACT:

Some soft sedimentary rocks, especially mudstones, are disintegrated or crumbled when subjected to cyclic drying and wetting, known as slaking. Drying/wetting and temperature variation are the influential factors in the slaking of mudstone. Therefore, a conventional oedometer was modified to make a drying/wetting cycle with temperature variation to examine the effects of slaking in four materials with different slaking ratios. Further, some mudstone, showing higher vertical strains along the drying/wetting cycle, was experimented with under the three loading conditions (100 kPa, 200kPa & 500 kPa) and different cycles. Penetration resistance and particle breakage were also measured after the oedometer test.

Key Words: *Slaking, Oedometer test, Slaking, Particle breakage, Penetration resistance.*

1. INTRODUCTION

Tertiary mudstone deposits with slaking nature extensively cover Japan's coastal and mountainous areas and are the most often encountered geologic material in excavation (Yoshida et al., 2002). Thus, in consideration of environmental and economic issues, it has been suggested using such mudstones as a construction material, particularly for earth structures or filling.

The strength and deformation characteristics of soft rocks, especially mudstone, deteriorate when the material are exposed to drying/wetting cycles, known as slaking, which was the cause of severe slope failures and ground settlements in several case studies (Nakano, 1967; Takagi, 2010; Yagiz, 2011). Further, some residential buildings built on the mudstone filling were tilted by differential settlement, caused by particle breakage and slaking (Mochizuki, et al., 1985).

The effect of temperature variation in slaking on mudstone has been observed by several researchers (Paaswell, 1967; Towhata et al., 1993). Additionally, the coupling effect of the drying/wetting with temperature (higher temperature in drying and lower temperature in wetting) caused a severe effect on volume changes in slaking material, observed by (Zhang et al., 2012; Zhang et al., 2015). However, particle breakage and shear strain along drying/wetting cycles are not comprehensively discussed in the

¹ Graduate Student, Dept. of Civil Eng. University of Tokyo

² Associate Professor, Institute of Industrial Science, University of Tokyo

³ Assistant Professor, Institute of Industrial Science, University of Tokyo

⁴ Senior Technical Specialist, Institute of Industrial Science, University of Tokyo

literature.

Therefore, this research targets to investigate the coupling effect of slaking, caused by drying/wetting with temperature variations cycle, on 1D deformation, particle breakage, and penetration resistance. A modified oedometer apparatus was developed and enhanced to make drying/wetting with temperature variants cycle.

2. MATERIAL

The gravelly mudstones used in this study were collected from several sites at Hamamatsu, and Okinawa in Japan, and Hattian Bala in Pakistan. For comparison, a non-slakable gravel material was tested to distinguish the slaking effect on the 1D deformation behavior of the sample. The physical properties of the tested materials are shown in Table 1. The collected sample was crumbled into relatively smaller particles to increase the surface area (so as to accelerate the slaking) and reduce the specimen's height: maximum particle size ratio to avoid arch formation (Mokhtari et al., 2015). For further details on particle size and specimen preparation, refer to Kiyota et al. (2011), Sawatsubashi et al. (2021), and Sharma et al. (2017).

The dry specimen (with a diameter $\phi=150\text{mm}$ and height $h=150\text{ mm}$) was prepared into the mold in five layers by external vibration (applied by a wooden hammer) to avoid particle breakage during sample preparation. Compaction was done by giving 20 hits at the outer surface of the mold for every layer to maintain a constant compaction energy for all materials.

Table 1: Four different materials' physical properties

Material	Slaking index ^{1*}	Slaking durability ^{2*}		Slaking ^{3*} ratio (%)	Specific density (g/cm ³)	Maximum dry density (proctor) ρ_{damx} (g/cm ³)	Wabs (%)
		Id 1 (%)	Id 2 (%)				
Hamamatsu	3	92.13	73.75	55.50	2.690	1.65	12.7
Okinawa	4	81.25	61.21	73.71	2.650	1.39	45.0
Hattian Bala	2	99.35	98.59	3.10	2.780	1.74	3.0
Non-slaking gravel	0	100	100	0.00	2.702	1.91	0.6

^{1*} (JGS, 2124),
^{2*} (Slaking Durability Index (ASTM D4544, 2016),
^{3*} (JHS110-2015), here in this Test, a 300-g dry specimen (with particle size of 19.5–37.5 mm) underwent one repeated cycle of drying (24 h) followed by immersion (24h). Then, the dry mass of the specimen was sieved by a 9.5-mm sieve; the percentage of the dry weight of passing the material through that sieve was defined as the slaking ratio.

3. APPARATUS AND TEST PROCEDURES

3.1. Modified oedometer test

In order to investigate the 1D deformation characteristics of gravelly mudstone subjected to drying/wetting cycles, a modified oedometer apparatus was developed. Its schematic diagram is shown in Fig. 1(a). The modified oedometer apparatus, additionally, consists of the drying/wetting system.

3.2. Drying/wetting system

A water tank was connected to the bottom of the specimen. Then water was allowed to flow upward into the specimen to wet the specimen until the vertical strain was settled (which was calibrated as 6 hours). The drying was done by wrapping a heater around the specimen mold and circulating dry air into the specimen. A thermometer was inserted inside the specimen for calibration, and the heater's temperature was changed (at the outer surface). An average specimen temperature of 56 °C was achieved during the drying stage, which was limited to 56 °C to avoid any unrealistic chemical reaction in the sample (Zhang et al., 2012). The vertical strain was continuously measured by an External Displacement Transducer (EDT). Time for drying up to less than 1% of moisture content was calibrated (as 48 hours) by inserting a moisture sensor into the mold, and the calibration curve of three different materials (water content reduction vs. time) was presented in Fig. 1(b). Further procedure and calibration had been explained in Nihaaj et al. (2021), and this comprehensive dry and wet cycle (6 hours wetting and 48 hours drying as mentioned earlier) hereinafter is called the D/W cycle in this paper.

3.3. Experimental set-up

i) Oedometer test

Four specimens, H-200-9, OKI-200-9, HB-200-9, and NSG-200-9, as shown in Table 2, were prepared using four materials: Hamamatsu mudstone, Okinawa mudstone, Hattian Bala mudstone, and non-slaking gravel respectively. First, these four specimens were subjected to 200 kPa vertical stress (σ_v) and 9 D/W cycles in the modified oedometer. Then, this series of experiments was extended for another two vertical stress conditions (100, and 500 kPa) for Hamamatsu mudstone. The details of this series are summarized in Table 2.

ii) Penetration resistance

Laboratory penetration tests were carried out to evaluate the effect of the D/W cycles on the strength characteristics of the specimen, which were tabulated in Table 2 (penetration resistance measured samples are indicated as Pen in the Note column).

The penetration resistance and penetration depth were monitored by a load cell and an EDT, respectively. A metal stick with a diameter of 3 mm, 60° apex angle, and a length of 150 mm was mounted below a load cell. Mold-to-stick diameter ratio was kept as 50 to reduce the rigid boundary effect, that could be caused by oedometer mold (Monfared, 2014; Pournaghiazar et al., 2011). The penetration test was done at 0.15 mm/sec, lower than ASTM D5778-2012 requirement, where the allowable is 20 mm/s, to reduce the particle size effect (Kokusho et al., 2003). The penetration test was done to an approximate depth of 100 mm from the top. The results are intended to represent the penetration strength qualitatively along with the D/W cycles.

iii) Particle breakage

In oedometer test, the particle breakage is impossible to be measured along the D/W cycle. So, different D/W cycles (0, 1, 5, & 9) were applied in different vertical stress conditions (100, 200 & 500 kPa) on Hamamatsu mudstone. At the end of the respective cycles, the remaining material in the mold was sieved to calculate the particle breakage. This experiment's conditions were explained in Table 2 as Br in the Note column. After the respective D/W cycles, the relative particle breakage index (Br), proposed by (Hardin., 1985), was evaluated.

Table 2 Experimental set-up of oedometer tests

Sample name	Degree of compaction (Dc)**	Vertical stress σ_v (kPa)	D/W cycle	Note
H-200-9	78	200	9	Br/Pen
HB-200-9	85	200	9	
OKI-200-9	78	200	9	
NSG-200-9	92	200	9	
H-100-9	78	100	9	Br/Pen
H-500-9	78	500	9	Br/Pen
H-100-0	78	100	0	Br
H-200-0	78	200	0	Br
H-500-0	78	500	0	Br
H-200-1	78	200	1	Br/Pen
H-200-5	78	200	5	Br/Pen
H-100-1	78	100	1	Br/Pen
H-100-5	78	100	5	Br/Pen
H-500-1	78	500	1	Br/Pen
H-500-5	78	500	5	Br/Pen

Br- After the D/W cycle, the specimen was sieved, and Relative Breakage (Br) was calculated
Pen- Needle penetration test conducted.

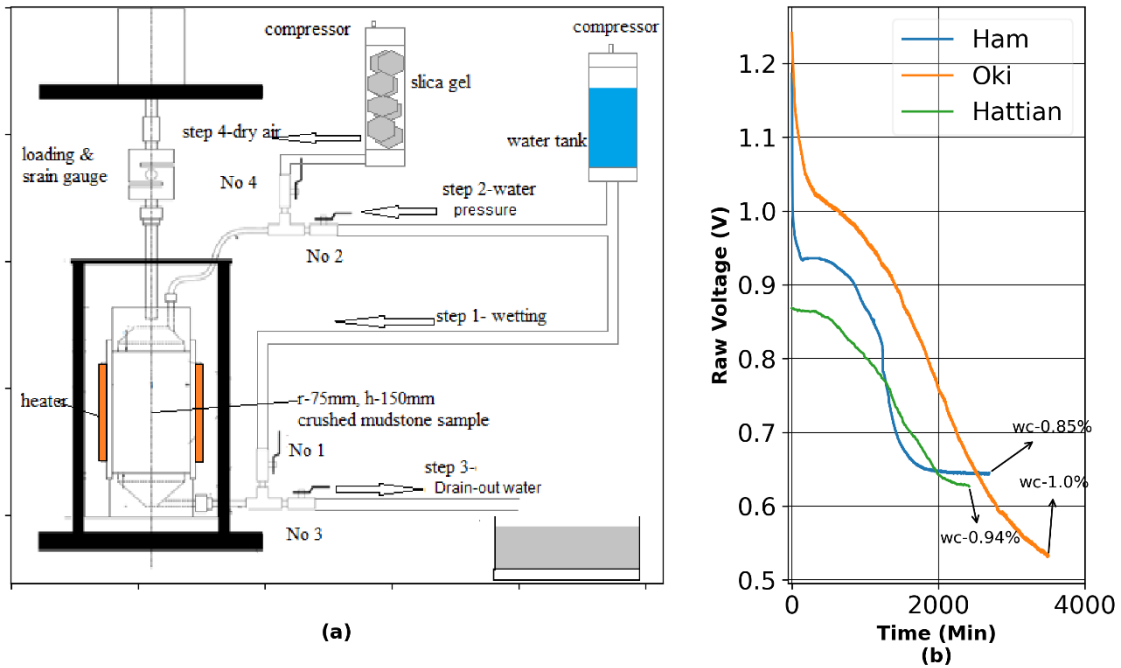


Fig. 1 (a) Schematic diagram of Modified oedometer, (b) Raw voltage/water content (%) vs. time at calibration

4. TEST RESULTS

4.1. Oedometer test

Fig. 2 (a) illustrates the vertical strain (ϵ_v) changes of four different materials at the 200 kPa vertical stress conditions. In Fig. 2(a), the hollow circles represent the dried and heated states (56 °C), whereas the solid circles represent the wetted at 20°C. The Okinawa (OKI-200-9) and Hamamatsu (H-200-9) mudstone showed more significant vertical strain (ϵ_v) development along the D/W cycle, up to 35% and 17.5%, respectively, compared with the other specimens prepared using Hattian Bala (HB-200-9) or non-slakable gravel (NSG-200-9), showing the vertical strain (ϵ_v) less than 5% at the end of the 9th cycle. Both OKI-200-9 and H-200-9 which showed severe increment at the first wetting due to the dried and pebble state of the initial condition and collapse behavior. Then, the increment in vertical strain (ϵ_v) was reduced along the D/W cycles and became flat after a few D/W cycles.

Fig. 2(b) explains the vertical strain (ϵ_v) changes of the Hamamatsu mudstone under the three different vertical stress conditions ($\sigma_v=100, 200, \text{ and } 500 \text{ kPa}$). The first wetting caused a large ϵ_v for all specimens prepared by Hamamatsu mudstone, and the increment of ϵ_v gradually decreased after that. However, minor variations in vertical strain (ϵ_v) were also observed during the drying and wetting state because wetting and drying showed swelling and contraction behavior, respectively. After the 8th cycle, none of these stress conditions further showed vertical strain (ϵ_v) development.

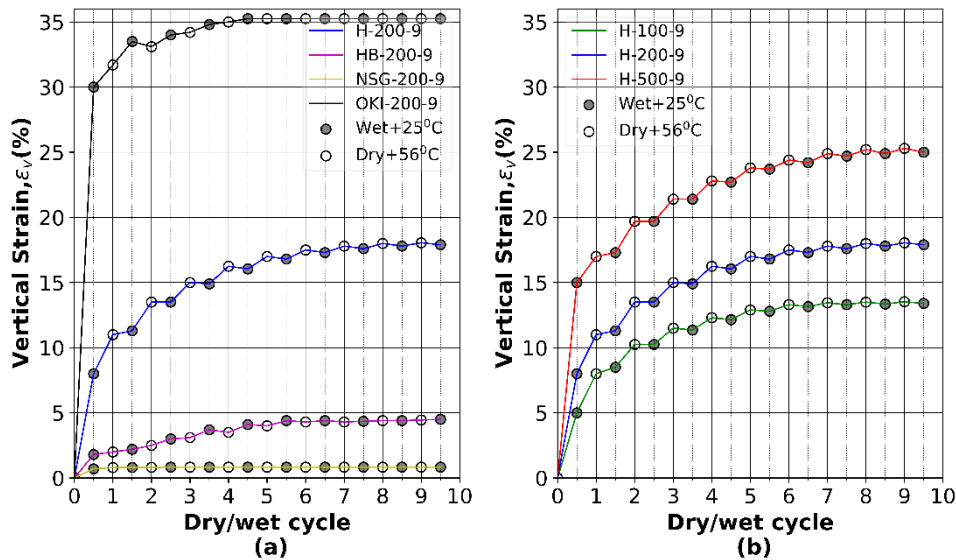


Fig. 2 Vertical strain (ϵ_v) vs. D/W- cycle of (a) four different mudstones at 200 kPa vertical stress, and (b) Hamamatsu mudstone at different vertical stress

4.2. Penetration resistance

Figs. 3 (a), (b), and (c) show the penetration resistance along the depth of the specimen after the 1st, 5th, and 9th D/W cycles in 100, 200, and 500 kPa vertical stress conditions, respectively. The penetration resistance increased with the depth due to the increased confinement and the needle's surface area

exposed to soil friction in all stress conditions. Furthermore, the resistance increased with increasing D/W cycles due to the densification until the 5th D/W cycle in all vertical stress conditions. However, an increment in penetration resistance after the 9th D/W cycle was only observed in 500 kPa condition (H-500-9 in Fig. 3(c)) than respective 5th D/W cycles (H-500-5 in Fig. 3(c)). Conversely, penetration resistance of the 9th D/W cycle at 100 and 200 kPa vertical stress conditions (H-100-9 and H-200-9 in Figs. 3(a) and (b) respectively) did not show any apparent increases compared with the respective 5th D/W cycle (H-100-5 and H-200-5 in Figs. 3(a) and (b) respectively).

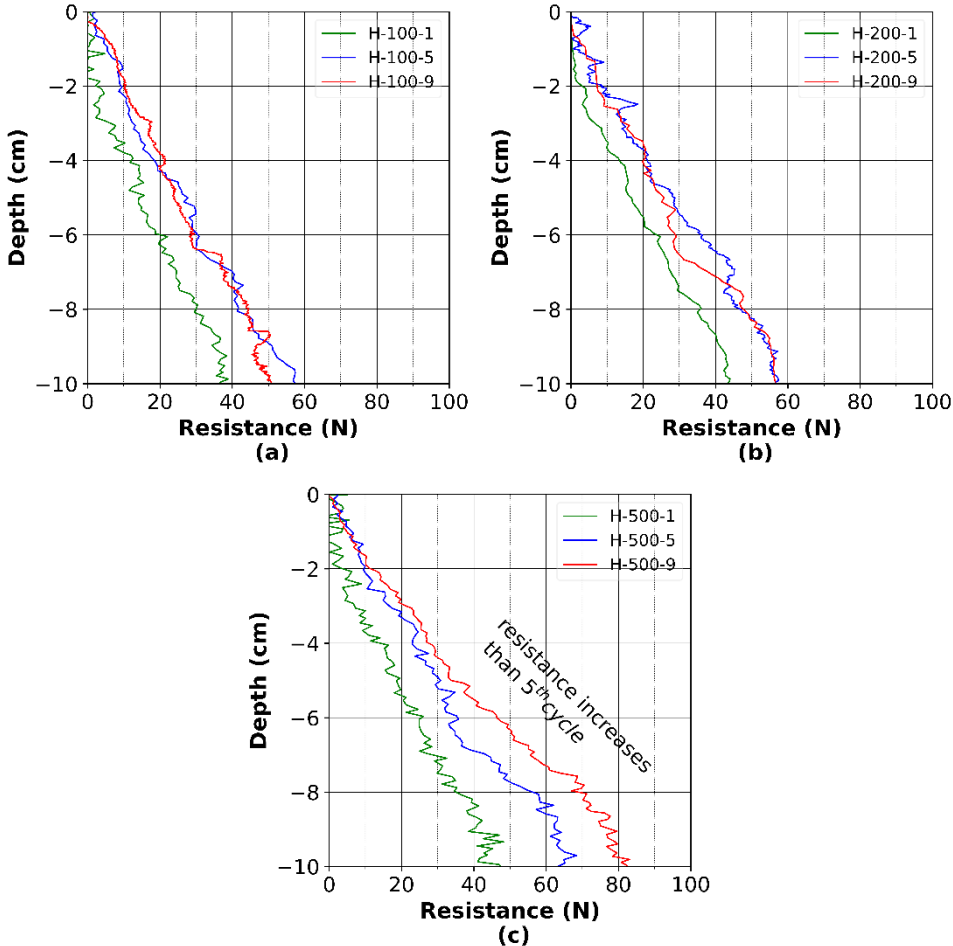


Fig. 3 Penetration resistance of (a) 100 kPa, (b) 200 kPa, and (c) 500 kPa after 1st, 2nd, and 5th D/W-cycle

4.3. Particle breakage

Fig. 4(a) shows the relative particle breakage (Br) (quantified by Hardin (1985)) of the samples after the loading (0-cycle), 1st, 5th, and 9th D/W-cycles under various σ_v conditions, as per explained in Table 2. The Br increased along with the increment of the D/W-cycles in all samples. After the 1st D/W cycle, the Br at 500 kPa stress condition is higher than other stress conditions (100 and 200 kPa). However, after the 5th and 9th D/W cycles, the 500 kPa stress sample showed lower Br. Conversely, the lower stress condition (100 kPa) showed lower Br after the 1st D/W cycle but higher Br at the 9th D/W cycle.

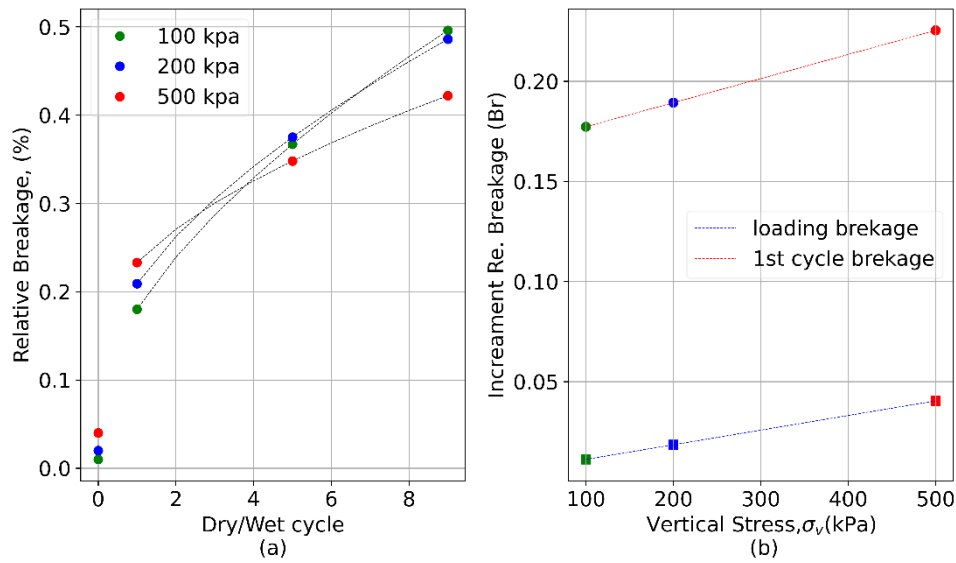


Fig. 4 (a) Relationship of Relative Breakage (Br) vs. the D/W cycle, (b) Relationship of increment of breakage vs. vertical stress at loading and 1st D/W cycle

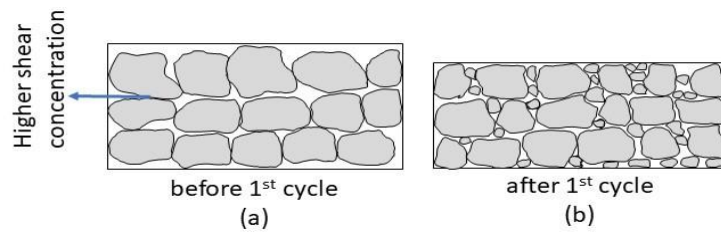


Fig. 5 Particle arrangement (a) Before 1st D/W cycle and (b) After 1st D/W cycle

5. DISCUSSION

Fig. 4(b) explains the Br increment after loading and 1st D/W cycle, where the Br increment and the vertical stress (σ_v) show the linear relationship. Figs. 5(a) and (b) explains particle arrangement before and after the 1st D/W cycle respectively.

Even though the specimen was loaded in 1D condition, shear stress concentration could be developed in particle contact as per Fig. 5(a). In the first cycle, shear stress concentration at the particle contact was high due to the initial lower density and narrow range of particle size (2-4.75mm) (lower particle contact). Therefore, particles can be softened due to swelling at the wetting state, as observed in heavily over-consolidated clays, which causes severe breakage (Nakano et al., 1998). So vertical stress (σ_v) and shear concentration in between the particles are the governing factors on the increment of breakage at the first cycle. Therefore, the vertical stress (σ_v) and increment of breakage showed the linear relation in Fig. 4(b).

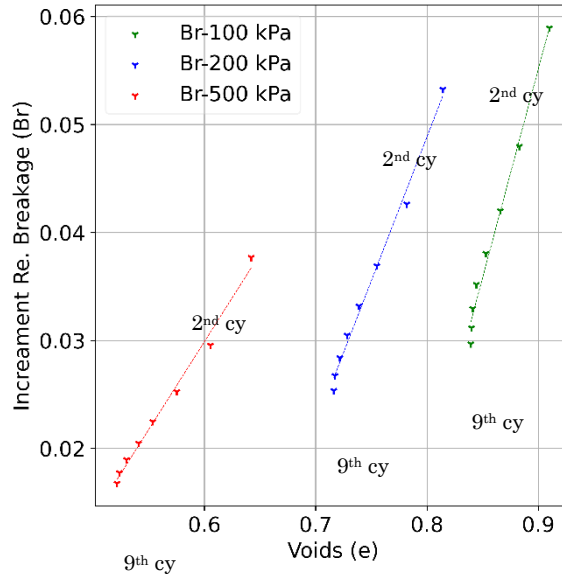


Fig. 6. Relationship of increment of breakage vs. voids at continuing D/W cycle (2 to 9 D/W cycle)

Fig. 6 explains the increment of the Br after the first cycle (2 to 9 D/W cycles). As per Nakano et al. (1998), this phenomenon of shear concentration is not significant at a denser state, where the particle contact increases, and the shear concentration is significantly reduced as per illustrated in Fig 5(b). Thus, voids became the governing factor over the shear stress concentration along the D/W cycles. An increment in voids increases the water contact with particles, which causes the particle breakage in continuing D/W cycles. Thus, smaller stress conditions (100 kPa) showed an increasing breakage trend than higher stress conditions (500 kPa). Increment of particle breakage could be influenced by vertical stress (σ_v) and void (e) of the specimen; thus, three trends in Fig. 6 could be observed with the vertical stress (σ_v) conditions. The void reduction was increased severely in higher stress conditions resulting in lower breakage increment in continuing D/W cycles.

The penetration resistance of the miniature rods is influenced by density and particle size (George & Nikolaos., 2003). An increase in density and particle size could increase the penetration resistance. Fig. 7 shows the relationship between the vertical strain (ϵ_v) and the Br in all stress conditions. Along the D/W cycle, the Br exponentially increased over vertical strain (ϵ_v). This exponential increment was very high in the lower vertical stress conditions (100 and 200 kPa) than in the higher stress condition (500 kPa). Even though the particle size was reduced along the D/W cycle, specimen density was increased. Increasing density is the governing factor rather than reducing particle size in the penetration resistance up to the 5th D/W cycles. The vertical strain (ϵ_v) did not increase in lower vertical stress conditions (100 and 200 kPa) after the 5th D/W cycle, as shown in Fig.7. Thus, the influence of the density increment was severely limited in lower stress conditions (100 and 200 kPa), which decreased the penetration resistance at the 9th D/W cycle (Fig. 3 (a)-H-100-9 and Fig. 3 (b)-H-200-9). But the higher vertical stress condition (500 kPa) showed substantial increases in the vertical strain (ϵ_v) (density) up to the 9th D/W cycle. So, penetration resistance of the 9th cycle at the higher vertical stress (Fig. 5 H-500-9) has shown an increment in penetration resistance.

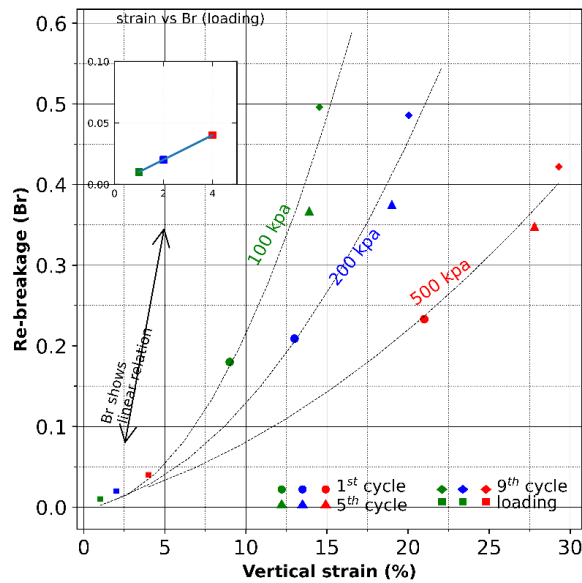


Fig. 7 Relationship of Vertical strain (ϵ_v) (%) vs. Relative Breakage (Br) in different vertical stress.

6. CONCLUSION

The vertical strain (ϵ_v) was evaluated among the mudstones with different physical properties along the D/W-cycle. The results showed a severe increment of vertical strain (ϵ_v) in the material with a higher slaking ratio. The particle breakage (Br) along D/W-cycle depended on two factors, vertical stress, and voids. At the first D/W-cycle, vertical stress was the governing parameter. However, at continuing D/W-cycle, voids became the governing factor. The penetration resistance depended on two factors, density, and particle size. At continuing D/W-cycle, there was a trade-off between density and particle size.

Reference

- ASTM, A. S. T. M. (2016). Standard Test Method for Slake Durability of Shales and Other Similar Weak Rocks. *ASTM International*. <https://doi.org/10.1520/D4644-16>
- George.k, & Nikolaos, G. . . (2003). Empirical correlations of soil parameters based on cone penetration test (CPT) fro Greek soil. *Geotechnical and Geological Engineering*, 40(2), 50–62. <https://doi.org/10.1023/B>
- JGS (Japanese Geotechnical Society). (2009). *JGS 2125-2009: Method for accelerated rock slaking Test*.
- Kiyota, T., Sattar, A., Konagai, K., Kazmi, Z. A., Okuno, D., & Ikeda, T. (2011). Breaching failure of a huge landslide dam formed by the 2005 Kashmir earthquake. *Soils and Foundations*, 51(6), 1179–1190. <https://doi.org/10.3208/sandf.51.1179>
- Kokusho, T.Murahata, K. Hushikida, T. and Ito, N. (2003). Introduction of miniature cone in triaxial apparatus and correlation with liquefaction strength. *Proceeding of the Annual Convention of Japan Society of Civil Engineering (JSCE), Tokyo, Japan, III-96, Japan Society for Civil Engineering, 191-192 (in Japanese)*.
- Mochizuki, A., Mikasa, M., and Kawamoto, S. (1985). "Investiga- tion of Settlement of Clay Fill at a Housing Development Site," (in Japanese) Title. *Tsuchi-To-Kiso, Vol. 33, No. 4, 1985, Pp. 25–32.No.*

- Mokhtari, M., Shariatmadari, N., Heshmati R, A. A., & Salehzadeh, H. (2015). Design and fabrication of a large-scale oedometer. *Journal of Central South University*, 22(3), 931–936. <https://doi.org/10.1007/s11771-015-2603-x>
- Monfared, S. D. (2014). Miniature Cone Penetration Test on Loose Sand. *Master Thesis, December*.
- Nakano, R. (1967). On weathering and change of properties of tertiary mudstone related to landslide. *Soils and foundations*, 7(1), 1–14. <https://doi.org/10.3208/sandf1960.7.1>
- Nihaaj, M., Kiyota, T., & Chua, M. G. (2021). *Internal erosion of gravelly mudstone due to drying / wetting and hydraulic pressure cycles in oedometer test* . 1–14.
- Hardin. B. (1985). Crushing of Soil Particles. *Journal of Geotechnical Engineering*, 111(10), 1177–1192. [https://doi.org/10.1061/\(ASCE\)0733-9410\(1985\)111:10\(1177\)](https://doi.org/10.1061/(ASCE)0733-9410(1985)111:10(1177))
- Paaswell, R. E. (1967). Temperature Effects on Clay Soil Consolidation. *Journal of the Soil Mechanics and Foundations Division*, 93(3), 9–22.
- Pournaghiazar, M., Russell, A. R., & Khalili, N. (2011). Development of a new calibration chamber for conducting cone penetration tests in unsaturated soils. *Canadian Geotechnical Journal*, 48(2), 314–321. <https://doi.org/10.1139/T10-056>
- Sakai, T., & Nakano, M. (2019). Effects of slaking and degree of compaction on the mechanical properties of mudstones with varying slaking properties. *Soils and Foundations*, 59(1), 56–66. <https://doi.org/10.1016/j.sandf.2018.09.004>
- Sawatsubashi, M., Kiyota, T., & Katagiri, T. (2021). Effect of initial water content and shear stress on immersion-induced creep deformation and strength characteristics of gravelly mudstone. *Soils and Foundations*, 61(5), 1223–1234. <https://doi.org/10.1016/j.sandf.2021.06.015>
- Sharma, K., Kiyota, T., & Kyokawa, H. (2017). Effect of slaking on direct shear behaviour of crushed mudstones. *Soils and Foundations*, 57(2), 288–300. <https://doi.org/10.1016/j.sandf.2017.03.006>
- Takagi, M. (2010). The actual situation of the slope of earth fill that collapsed by an earthquake disaster in the Tomei Expressway Makinohara district. *J. Geotech. Eng. Symp., JGS*, 55(29), 193–196.
- Towhata, I., Kuntiwattanaku, P., Seko, I., & Ohishi, K. (1993). Volume Change of Clays Induced by Heating as Observed in Consolidation Tests. *Soils and Foundations*, 33(4), 170–183. https://doi.org/https://doi.org/10.3208/sandf1972.33.4_170
- Yagiz, S. (2011). Correlation between slake durability and rock properties for some carbonate rocks. *Bulletin of Engineering Geology and the Environment*, 70(3), 377–383. <https://doi.org/10.1007/s10064-010-0317-8>
- Yoshida, N., Enami, K., & Hosokawa, K. (2002). Staged compression-immersion direct shear test on compacted crushed mudstone. *Journal of Testing and Evaluation*, 30(3), 239–244. <https://doi.org/10.1520/jte12311j>
- Zhang, B. Y., Zhang, J. H., & Sun, G. L. (2012). Particle breakage of argillaceous siltstone subjected to stresses and weathering. *Engineering Geology*, 137–138, 21–28. <https://doi.org/10.1016/j.enggeo.2012.03.009>
- Zhang, C. L., Wicczorek, K., & Xie, M. L. (2010). Swelling experiments on mudstones. *Journal of Rock Mechanics and Geotechnical Engineering*, 2(1), 44–51. <https://doi.org/https://doi.org/10.3724/SP.J.1235.2010.00044>
- Zhang, D., Chen, A., Wang, X., & Liu, G. (2015). Quantitative determination of the effect of temperature on mudstone decay during wet-dry cycles: A case study of "purple mudstone" from south-western China. *Geomorphology*, 246, 1–6. <https://doi.org/10.1016/j.geomorph.2015.06.011>